Engineering Chemistry
ISSN: 2813-6535, Vol. 5, pp 49-56
doi:10.4028/p-i1dZ9Z

Submitted: 2023-03-31
Revised: 2023-07-06
Accepted: 2023-07-14
Online: 2024-01-19

The Effect of Nitrogen on the Capacitive Properties of N-Doped rGO/$CuCr_2O_4$ Composites as Materials for Supercapacitors

Diah Susanti[1,a*], Adzon Nugraha Rizky Pratama[1,b] and Haniffudin Nurdiansah[1,c]

[1]Materials and Metallurgical Engineering Department, Institut Teknologi Sepuluh Nopember (ITS), Surabaya, Indonesia

*Corresponding author email: [a]santiche@mat-eng.its.ac.id, [b]adzonnrp@gmail.com, [c]haniffudin@mat-eng.its.ac.id

Keywords: Hydrothermal, Specific Capacitance, N-Doped rGO/$CuCr_2O_4$ composite, Hybrid Supercapacitor

Abstract. A hybrid supercapacitor is an energy storage device that combines the properties of EDLCs and pseudocapacitors. In this research, the goal was to analyze the effect of hydrothermal temperature on the structure, morphology, and capacitive properties of the N-Doped reduced graphene oxide/Copper Chromite (N-Doped rGO/$CuCr_2O_4$) composite, which was being investigated as a potential material for hybrid supercapacitor electrodes. The method used was hydrothermal, with temperature variations of 120°C, 140°C, and 160°C. The structure and morphology of the composites were analyzed using Scanning Electron Microscope (SEM) and Energy Dispersive X-Ray Analysis (EDX), X-Ray Diffractometer (XRD), and Fourier Transform Infrared Spectrometer (FTIR). Meanwhile, the capacitance and conductivity values of N-doped rGO/$CuCr_2O_4$ were measured using Cyclic Voltammetry (CV) and Electrochemical Impedance Spectroscopy (EIS) tests. The results of the XRD tests showed that an increase in temperature led to a greater $d_{spacing}$ value, indicating the presence of more substituted nitrogen atoms. This was supported by the results from EDX, which showed that the sample with a hydrothermal temperature of 160°C had the largest percentage of nitrogen. Nitrogen is important in increasing the conductivity of the material. The FTIR results revealed a covalent bond between Carbon (C) and Nitrogen (N). Meanwhile, the results of the CV test, performed at a scan rate of 5 mV/s and a potential window of 0-0.8 V, showed that the specific capacitance values were 99.5, 196.16, and 221.59 Fg^{-1} for the samples with hydrothermal temperatures of 120°C, 140°C, and 160°C, respectively. The EIS test measured the conductivity values of the samples, which were 0.123, 0.518, and 0.549 S/m for the samples with hydrothermal temperatures of 120°C, 140°C, and 160°C, respectively. Thus, the specific capacitance values were influenced by the electrical conductivity of the materials and the nitrogen doping content in the electrode composite material.

Introduction

Indonesia is working with the United Nations as part of the global effort to achieve the goals outlined in the Sustainable Development Goals (SDGs) framework. As part of this effort, the country is transitioning from fossil fuels to renewable energy sources for electricity generation, and reliable energy storage solutions are needed. Electrochemical supercapacitors are a promising option for energy storage.

Supercapacitors are among the top electrical energy storage technologies, offering advantages such as fast charging times, long life cycles, environmental sustainability, and high-temperature operation. There are three main types of supercapacitors: Electrochemical Double-Layer Capacitors (EDLCs), pseudocapacitors, and hybrid supercapacitors [1]. The capacitance of EDLCs can be increased by using materials with high surface areas, such as graphene [2], while the capacitance of pseudocapacitors can be boosted by combining carbon with pseudocapacitive materials, such as metal oxides.

Graphene is a crystalline form of carbon with a diamond-like crystal structure [3]. It boasts impressive physical properties, including a tensile strength of 130.5 GPa, Young's modulus of 1.0 TPa [4], low density (0.77 mg m^{-2}), a high specific area (up to 2630 m^2gr^{-1}), intrinsic mobility (up to 200,000 $cm^2V^{-1}s^{-1}$), and thermal conductivity (up to 5000 $Wm^{-1}K^{-1}$) [5].

A hybrid supercapacitor electrode with optimal capacitance can be achieved by combining the properties of EDLCs and pseudocapacitors. $CuCr_2O_4$ is a metal oxide commonly used in pseudocapacitor electrodes due to its capacitive properties, cyclic stability, and high-power density [6]. By combining rGO and $CuCr_2O_4$, a hybrid supercapacitor can be produced. Nitrogen doping of reduced graphene oxide (rGO) can effectively enhance its electronic properties by introducing an additional free electron into the carbon structure of rGO. This process not only alters the chemical composition but also influences the capacitive properties of N-doped rGO [7]. Therefore, this research aimed to examine the impact of hydrothermal temperature on the structure, morphology, and capacitive properties of the N-doped rGO/$CuCr_2O_4$ composite material as a hybrid supercapacitor.

Experiments

The synthesis process of $CuCr_2O_4$ was carried out by dissolving $CuSO_4$, $K_2Cr_2O_7$, and NH_4OH using distilled water and stirring for 30 minutes to achieve homogeneity. The resulting precipitate was filtered using filter paper and dried at 110 ºC for 12 hours. Calcination was then performed at a temperature of 500 ºC for 2 hours to obtain $CuCr_2O_4$ powder.

rGO was synthesized via a modified Hummer method. 2 g of graphite powder was stirred into 80 ml of 98% H_2SO_4 solution at an ice bath temperature (0-5 °C) for 4 hours. After 4 hours of stirring, 4 g $NaNO_3$, and 8 g $KMnO_4$ were gradually and alternately added to the solution. The stirring was continued at 35 °C for 20 hours outside the ice bath and then 200 ml of distilled water was gradually added and stirred for another hour until the solution became homogeneous.

The remaining $KMnO_4$ content in the solution was removed by adding of 20 ml of H_2O_2 and stirring for 30 minutes. The solution was then centrifuged for 1 hour at 2500 rpm and the precipitate was washed with 5% HCl (0.01 M) to remove the remaining metal ions. The washing process was repeated until the pH was neutral.

Nitrogen doping on rGO was performed using NH_4OH. 250 mg rGO and 2 mL of NH_4OH were mixed with 50 mL of distilled water in a 100 mL beaker glass. The mixture was ultra-sonicated for 30 minutes to facilitate the entry of H_2O and NH_4OH into the interlayer area of rGO. The mixture was then placed into a stainless-steel autoclave and hydrothermally treated in a furnace with temperature variations of 120º, 140º, and 160º C for 4 hours each, followed by drying for 12 hours.

The N-doped rGO/$CuCr_2O_4$ composite was synthesized using the sol-gel method. N-doped rGO and $CuCr_2O_4$ were ultrasonicated separately for 2 hours each, then mixed in a 95:5 ratio of N-doped rGO to $CuCr_2O_4$ and stirred at 500 rpm for 2 hours. The resulting precipitate was washed with distilled water until the pH was neutral and dried at 60°C for 12 hours. This process resulted in the formation of an N-doped rGO/$CuCr_2O_4$ composite.

A solution of N-doped rGO/$CuCr_2O_4$ composite and distilled water at a ratio of 1 mg of N-doped rGO/$CuCr_2O_4$ composite: 1 mL of distilled water was deposited on Nickel foam using ultrasonic for 90 minutes to form a working electrode of hybrid supercapacitor. The samples were dried at 110 °C for 12 hours, compressed, and weighed to measure the mass of the N-doped rGO/$CuCr_2O_4$ composite deposited on the Nickel Foam surface. The prepared electrodes were then tested using Cyclic Voltammetry (CV) instrument and Electrochemical Impedance Spectroscopy (EIS) with 1M Na_2SO_4 electrolyte solution.

The materials characterizations performed in this study included X-ray Diffraction (XRD), Fourier Transform Infra-Red (FTIR), Energy Dispersive X-Ray Analysis (EDX), Cyclic Voltammetry (CV), and Electrochemical Impedance Spectroscopy (EIS). Electrochemical measurements, specifically cyclic voltammetry (CV) and electrochemical impedance spectroscopy (EIS), were conducted using a three-electrode setup. The setup included the composite sample as the working

electrode, a graphite rod as the counter electrode, and a standard calomel electrode (SCE) as the reference electrode. CV measurements were performed within a potential window of 0-0.8 V at scan rates of 5, 10, 25, 50, and 100 mVs^{-1}. On the other hand, EIS tests were conducted at frequencies ranging from 0.1 to 10^5 Hz with an AC amplitude of 10 mV and a DC potential of 0 V. For ease in the designation, the composite treated at 120°C was labeled as N-rGO120, at 140°C was labeled as N-rGO140, and at 160°C was labeled as N-rGO160, and the electrodes were labeled as E120, E140, and E160.

Result and Discussion

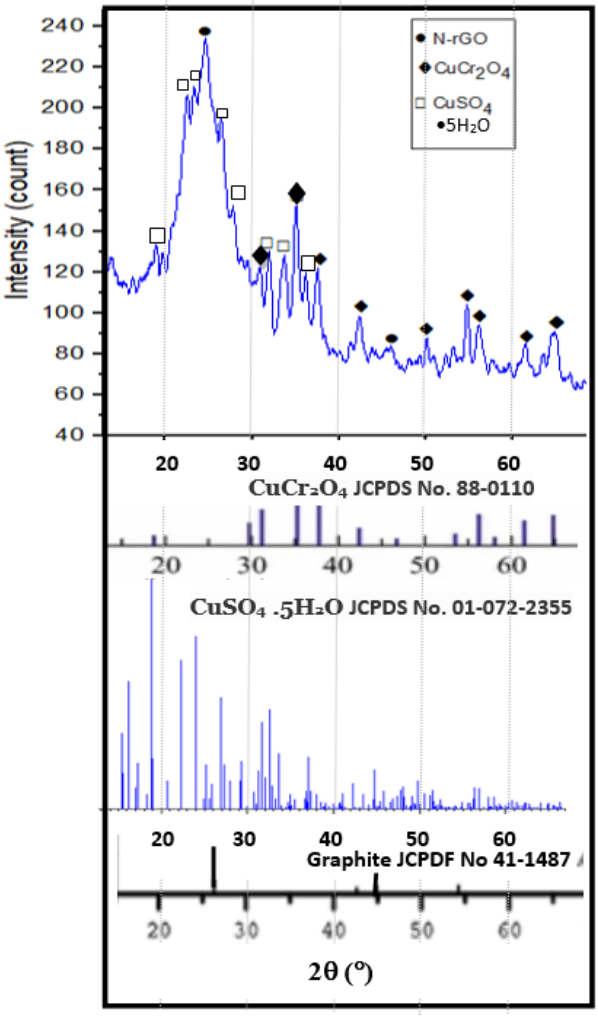

Fig. 1. X-Ray Diffraction pattern of N-rGO/$CuCr_2O_4$ composite material compared to standard XRD patterns of materials.

Fig. 1 displays the XRD pattern of the N-rGO/$CuCr_2O_4$ composite material. The peaks corresponding to N-rGO marked with solid circles can be seen at 2θ = ~24° and 2θ = ~43° (JCPDF No 41-1487) [8]. The XRD pattern displayed similarities to that of graphite; however, it exhibited an amorphous structure characterized by low intensities and broadened peaks. The XRD peaks of $CuCr_2O_4$, marked with diamond symbols, indicate a tetragonal structure (JCPDS No 88-0110) [9]. Additionally, the XRD pattern reveals the presence of $CuSO_4.5H_2O$ as an impurity (JCPDS No 01-072-2355) [10]. Using Bragg's Law, the $d_{spacing}$ of rGO, N-rGO120, N-rGO140, and N-rGO160 were 3.58, 3.59, 3.61, and 3.73 nm, respectively. Therefore, the $d_{spacing}$ increased as the hydrothermal temperature was raised, suggesting that more nitrogen atoms were incorporated into the carbon atom lattice arrangement at higher temperatures. As the lattice spacing expanded further at higher temperatures, more dopants could penetrate the material structure.

The crystallite sizes of rGO, N-rGO120, N-rGO140, and N-rGO160 were determined using the Debbye-Scherrer formula and found to be 94.43, 94.42, 94.39, and 94.25 Å, respectively. While the values were not significantly different, the crystallite sizes appeared to decrease slightly with increasing temperature.

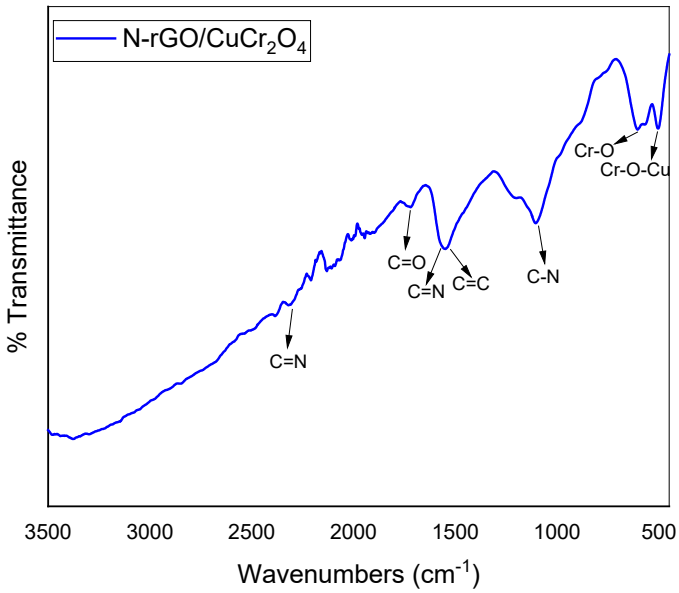

Fig. 2. FTIR result of N-rGO/$CuCr_2O_4$ composite material

Fig. 2 illustrates the results of the FTIR analysis performed on the N-rGO/$CuCr_2O_4$ composite material. The absorption peaks at 550 and 630 cm^{-1} are associated with the Cr-O-Cu and Cr-O vibrations of $CuCr_2O_4$, respectively, which has been previously reported [11]. Furthermore, other IR peaks were detected at 1100.19 cm^{-1}, 1535.34 cm^{-1}, 1565.7 cm^{-1}, 1725.97 cm^{-1}, and 2220 cm^{-1}, representing the C-N, C=C, C≡N, C=O, and C≡N bonds, respectively. The presence of C-N and C≡N peaks indicated Nitrogen doping in rGO, while the C=C and C=O peaks suggested the presence of rGO bonds.

Fig. 3 depicts the N-rGO/$CuCr_2O_4$ composite deposited on the surface of a nickel foam. The composite material effectively filled the pores of the nickel foam, promoting the smooth flow of electrons and ions.

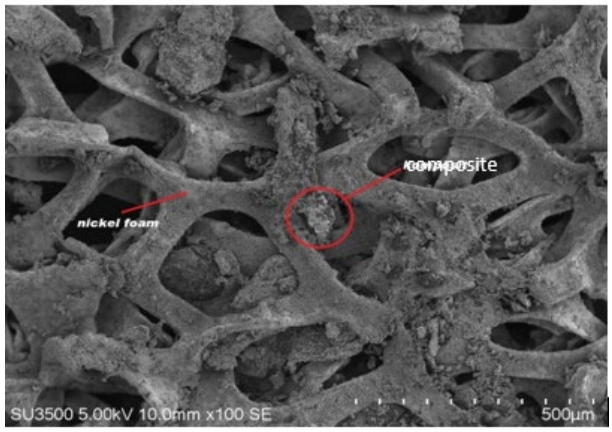

Fig. 3. N-rGO/ $CuCr_2O_4$ was deposited on Ni foam

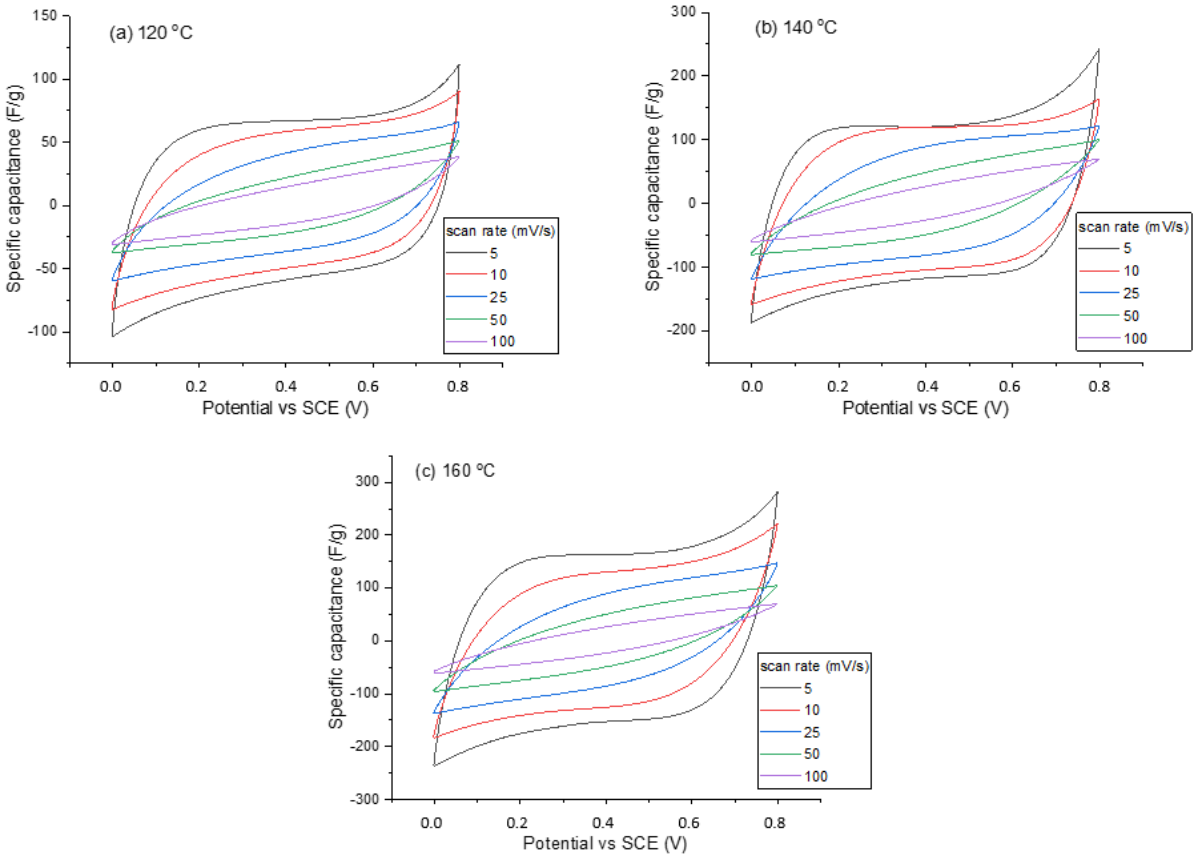

Fig. 4. Cyclic Voltammetry (CV) diagrams of N-rGO120, N-rGO140, and N-rGO160.

Figure 4 presents the CV curves normalized as specific capacitance (Fg^{-1}) vs. potential (V) at different scan rates of 5, 10, 25, 50, and 100 mVs^{-1}. As the scan rate increased, the CV curves and specific capacitances decreased. This decrease can be attributed to the fact that a slower scan rate allows more charges, in the form of electrons and ions, to be stored and released from less accessible sites within the hybrid supercapacitor electrode, leading to higher specific capacitances. All the CV diagrams exhibit almost symmetrical curves at the y-axis = 0 (0 Ampere current) and nearly horizontal rectangular shapes, indicating nearly ideal electrochemical supercapacitor behaviours.

Table 1 displays the specific capacitances, specific energy densities, and specific power densities of the electrodes at various scan rates. The electrode labelled as E160 exhibited the highest specific capacitances and specific energy densities, followed by samples E140 and E120. Interestingly, the specific power density values showed an inverse relationship to the specific energy density values. As the specific energy densities increased, the supercapacitor required more time to charge and discharge, resulting in lower power densities. It is important to note that power density is determined by dividing energy density by time.

The highest specific capacities at scan rate of 5 mVs^{-1} were 221.6 Fg^{-1}, 196.2 Fg^{-1}, and 99.5 Fg^{-1} for samples E160, E140, and E120 respectively. The specific capacitances of E160 ranged from 221.6 Fg^{-1} to 89.1 Fg^{-1} at scan rates ranging from 5 mVs^{-1} to 100 mVs^{-1}. Similarly, the specific capacitances of E140 ranged from 196.2 Fg^{-1} to 55.7 Fg^{-1}, while those of E120 ranged from 99.5 Fg^{-1} to 29.4 Fg^{-1}. It is worth noting that these values were found to be lower than those reported by Sarkar, et.al (2020) for supercapacitors made from the same composite material of N-rGO/$CuCr_2O_4$. Specifically, the specific capacitances at a scan rate of 2 mV s^{-1} and potential window of -0.2 V to 0.4 V were reported as 291.1, 825.6 and 290.6 Fg^{-1} for the composition ratios of N-rGO : $CuCr_2O_4$ 90:10, 95:5, and 98:2 respectively. However, our values were higher than those reported by Angelika, et.al (2022) who reported the highest specific capacitance of 36.86 Fg^{-1} for the same composite material at scan rate of 5 $mVs^{-1}$and potential window of 0 – 0.8 V [13].

Table 1. Specific Capacitance, Specific Energy Density, and Specific Power Density of The Samples based on the CV measurements

Sample	Scan rate (mVs^{-1})	Cs (Fg^{-1})	Specific Energy Density, W ($Whkg^{-1}$)	Specific Power Density, P (Wkg^{-1})
E120	5	99.5	8.8	99.8
	10	83.4	7.3	164.8
	25	59.7	5.3	298.4
	50	38.4	3.4	384.2
	100	29.4	2.6	587.8
E140	5	196.2	17.4	196.8
	10	168.5	14.9	336.9
	25	124.4	11.1	622.1
	50	82.9	7.4	829.3
	100	55.7	4.9	1113.5
E160	5	221.6	19.7	222.3
	10	192.7	17.1	385.4
	25	135.5	12	677.5
	50	89.1	7.9	891.4
	100	55.1	4.9	1101.5

Table 2 displays the $d_{spacing}$ based on XRD measurement, nitrogen content based on EDX, electrical conductivity based on EIS measurement, and specific capacitance based on EIS measurement. The EDX analysis results indicate that the N-rGO120 sample contained 11.74% nitrogen, while the N-rGO140 and N-rGO160 samples contained 12.9% and 14.88% nitrogen, respectively. These findings suggest that as the hydrothermal temperature increased, the nitrogen content in the composite material also increased. The higher temperature during the hydrothermal process likely provided more energy for the decomposition of nitrogen from NH_4OH and facilitated its insertion into the carbon lattice, leading to the increased nitrogen content in the composite material. This trend confirmed the XRD results written above, which indicated that as the temperature increased, the $d_{spacing}$ of carbon increased from 3.59 nm, 3.61 nm, to 3.73 nm, suggesting the insertion of more nitrogen into the carbon lattice. As the consequences, the electrical conductivities also increased from 0.123, 0.518, to 0.549 Sm^{-1}. The specific capacitance values were seemed to be determined by the electrical conductivities as shown from the CV measurements, in which the E160 showed the highest specific capacitances.

In table 2, the specific capacitance calculated based on EIS measurement at 0.1 Hz showed in-line trend with the results from CV measurement. The values of 33.6 Fg^{-1}, 115.6 Fg^{-1}, and 116.2 Fg^{-1} resulted from samples E120, E140, and E160, respectively, were comparable to those from CV measurements at 25-50 mVs^{-1}.

Table 2. $d_{spacing}$, nitrogen content based on EDX, electrical conductivity based on EIS measurement, and specific capacitance based on EIS measurement

Sample	$d_{spacing}$ (nm) (XRD)	Nitrogen Content (%) (EDX)	Conductivity (Sm^{-1}) (EIS)	Specific Capacitance (Fg^{-1}) (EIS)
E120	3.59	11.74	0.123	33.6
E140	3.61	12.9	0.518	115.4
E160	3.73	14.88	0.549	116.2

Summary

In conclusion, this study found that increasing the hydrothermal temperature led to a reduction in rGO, decreased the crystal size, and increased the $d_{spacing}$ value, indicating successful nitrogen substitution. This was confirmed by the EDX test, which showed the highest nitrogen content of 14.88% in the sample treated at a hydrothermal temperature of 160°C. The results of the CV and EIS tests showed that the hybrid supercapacitor electrode (N-rGO/$CuCr_2O_4$) combined the characteristics of EDLC and pseudocapacitors, confirming the successful formation of the hybrid supercapacitor electrode. The highest capacitance value observed in the E160 sample was 221.59 F/g at 5 mVs^{-1} scan rate due to the highest conductivity value of 0.549 Sm^{-1}.

Acknowledgment

This work was financially supported by the Directorate of Research and Community Service (DRPM), Sepuluh Nopember Institute of Technology (ITS). The authors also acknowledge the facilities, scientific and technical support from Materials Chemistry Laboratory, Corrosion, and Material Failure Laboratory, and Materials Characterization Division, Department of Materials and Metallurgical Engineering – ITS.

References

[1] H. Lund, Renewable energy strategies for sustainable development, Energy. 32:6 (2007) 912–919 doi: 10.1016/j.energy.2006.10.017.

[2] V. D. Nithya, A review on holey graphene electrode for supercapacitor, J. Energy Storage. 44:PB (2021) 103380. doi: 10.1016/j.est.2021.103380.

[3] A. González, E. Goikolea, J. A. Barrena, and R. Mysyk, Review on supercapacitors: Technologies and Materials, Renew. Sustain. Energy Rev. 58(2016) 1189–1206. doi: 10.1016/j.rser.2015.12.249.

[4] G. A. Ferrero, A. B. Fuertes, and M. Sevilla, N-doped porous carbon capsules with tunable porosity for high-performance supercapacitors, J. Mater. Chem. A. 3:6 (2015) 2914–2923. doi: 10.1039/c4ta06022a.

[5] A. U. Sokolnikov, Graphene for Defense and Security. RC Press, Boca Raton-Florida, ISBN: 1351646680, 9781351646680, 2017.

[6] C. Lee, X. Wei, J. W. Kysar, and J. Hone, Measurement of the elastic properties and intrinsic strength of monolayer graphene, Sci. 321:5887 (2008) 385–388. doi: 10.1126/science.1157996.

[7] Y. Zhu and S. Murali., Graphene and graphene oxide: Synthesis, properties, and applications, Adv. Mater. 22:35 (2010) 3906–3924. doi: 10.1002/adma.201001068.

[8] L. Ma, Z. Wang, S. Tian, X. Liu, Z. Li, J. Huang, D. Xiyu, and Y. Huang, The αFe_2O_3/graphite anode composites with enhanced electrochemical performance for lithium-ion batteries, Nanotech. 31:43 (2020) 435404. doi: 10.1088/1361-6528/aba3a0

[9] J. Safaei-Ghomi, Z. Akbarzadeh, and B. Khojastehbakht-Koopaei, C–N cross-coupling reaction catalysed by reusable $CuCr_2O_4$ nanoparticles under ligand-free conditions: a highly efficient synthesis of triarylamines, RSC Adv. 3:37 (2015) 28879-28884. doi: 10.1039/C5RA01915J

[10] F. Fitrony, R. Fauzi, L. Qadariyah, and M. Mahfud, Pembuatan Kristal Tembaga Sulfat Pentahidrat ($CuSO_4.5H_2O$) dari Tembaga Bekas Kumparan, Jurnal Teknik ITS. 2:1 (2013) F121-F125. doi: 10.12962/j23373539.v2i1.2349

[11] M. H. Habibi and F. Fakhri, Fabrication and Characterization of $CuCr_2O_4$ Nanocomposite by XRD, FESEM, FTIR, and DRS, Synth. React. Inorganic, Met. Nano-Metal Chem. 46:6 (2016) 847–851. doi: 10.1080/15533174.2014.989591.

[12] S. Sarkar, R. Akshaya, and S. Ghosh, Electrochimica Acta Nitrogen doped graphene/$CuCr_2O_4$ nanocomposites for supercapacitors application : Effect of nitrogen doping on coulombic efficiency, Electrochim. Acta. 332 (2020) 135368. https://doi.org/10.1016/j.electacta. 2019.135368

[13] S. Angelika, D. Susanti, and Nurdiansah, H, Analisis Pengaruh Komposisi Material Komposit terhadap Sifat Kapasitif Superkapasitor Berbahan N-doped rGO/$CuCr_2O_4$, Undergraduate Thesis, Department of Materials and Metallurgical Engineering Department, Institut Teknologi Sepuluh Nopember (ITS), Surabaya-Indonesia, 2022.